Swansea University
Prifysgol Abertawe

Cronfa
Setting Research Free

Cronfa - Swansea University Open Access Repository

This is an author produced version of a paper published in:
Sustainable Energy & Fuels

Cronfa URL for this paper:
http://cronfa.swan.ac.uk/Record/cronfa38522

Paper:
Barbe, J., Kumar, V., Newman, M., Lee, H., Jain, S., Chen, H., Charbonneau, C., Rodenburg, C. & Tsoi, W. (2018). Dark electrical bias effect on moisture-induced degradation in inverted lead halide perovskite solar cells measured by advanced chemical probes. *Sustainable Energy & Fuels*
http://dx.doi.org/10.1039/C7SE00545H

This item is brought to you by Swansea University. Any person downloading material is agreeing to abide by the terms of the repository licence. Copies of full text items may be used or reproduced in any format or medium, without prior permission for personal research or study, educational or non-commercial purposes only. The copyright for any work remains with the original author unless otherwise specified. The full-text must not be sold in any format or medium without the formal permission of the copyright holder.

Permission for multiple reproductions should be obtained from the original author.

Authors are personally responsible for adhering to copyright and publisher restrictions when uploading content to the repository.

http://www.swansea.ac.uk/library/researchsupport/ris-support/

Check for updates

View Article Online
View Journal

Sustainable Energy & Fuels

Accepted Manuscript

This article can be cited before page numbers have been issued, to do this please use: J. Barbe, V. Kumar, M. Newman, H. Lee, S. M. Jain, H. Chen, C. Charbonneau, C. Rodenburg and W. Tsoi, *Sustainable Energy Fuels*, 2017, DOI: 10.1039/C7SE00545H.

This is an Accepted Manuscript, which has been through the Royal Society of Chemistry peer review process and has been accepted for publication.

Accepted Manuscripts are published online shortly after acceptance, before technical editing, formatting and proof reading. Using this free service, authors can make their results available to the community, in citable form, before we publish the edited article. We will replace this Accepted Manuscript with the edited and formatted Advance Article as soon as it is available.

You can find more information about Accepted Manuscripts in the author guidelines.

Please note that technical editing may introduce minor changes to the text and/or graphics, which may alter content. The journal's standard Terms & Conditions and the ethical guidelines, outlined in our author and reviewer resource centre, still apply. In no event shall the Royal Society of Chemistry be held responsible for any errors or omissions in this Accepted Manuscript or any consequences arising from the use of any information it contains.

ROYAL SOCIETY OF CHEMISTRY

rsc.li/sustainable-energy

View Article Online
DOI: 10.1039/C7SE00545H

Published on 12 February 2018. Downloaded on 12/02/2018 15:37:05.

Dark electrical bias effect on moisture-induced degradation in inverted lead halide perovskite solar cells measured by advanced chemical probes

Jérémy Barbé[†], *Vikas Kumar*[‡], *Michael J. Newman*[†], *Harrison K.H. Lee*[†], *Sagar M. Jain*[†], *Hu Chen*[§], *Cécile Charbonneau*[†], *Cornelia Rodenburg*[‡], *Wing C. Tsoi*[†]*

[†]SPECIFIC, College of Engineering, Swansea University, Bay Campus, Fabian Way, Swansea, SA1 8EN, U.K.

[‡]Department of Materials Science and Engineering, University of Sheffield, Mappin Street, Sheffield S1 3JD, U.K.

[§]KAUST Solar Center, Physical Science and Engineering Division, King Abdullah University of Science and Technology, Thuwal 23955-6900, Saudi Arabia

AUTHOR INFORMATION

Corresponding Author

*E-mail: W.C.Tsoi@Swansea.ac.uk

[†]Electronic supplementary information (ESI) available.

Sustainable Energy & Fuels Accepted Manuscript

View Article Online
DOI: 10.1039/C7SE00545H

Published on 12 February 2018. Downloaded on 12/02/2018 15:37:05.

ABSTRACT: Emerging lead halide perovskite materials have enormous potential for a range of optoelectronic devices, such as solar cells, light emitting diodes, transistors and lasers. However, the large-scale commercialization of these technologies will depend on the ability of the active material to be stable under environmental and operating conditions. In this work, we measured the first time the electrical bias-induced degradation of inverted perovskite solar cells in the dark in different environments and concluded that humidity coupled with electrical bias results in fast degradation of $CH_3NH_3PbI_3$ into PbI_2. Micro-Raman and photoluminescence show that the degradation starts from the edge of the cell due to moisture ingress. By using novel local Raman-transient photocurrent measurements, we were able to probe local ion migration at the degraded region and non-degraded region and found that the formation of PbI_2 can passivate perovskite by reducing ion migration. The degradation is far from uniform across different grains as revealed by secondary electron hyperspectral imaging, an advanced scanning electron microscopy technique which allows probing the composition of individual grain from the cross-section. By using potential step chronoamperometry, we also found that the bias degradation is closely related to the density of mobile ions. The unique combination of established methods with several novel analytical tools provides an insight into the origin of the bias-degradation of inverted perovskite solar cells from nano-scale to cell level, and demonstrates the potential of these novel tools for studying the degradation in other perovskite systems.

Introduction

Since their invention in 2009[1], organometal halide perovskite solar cells (PSCs) have shown unprecedented performance improvements, now exceeding 22% power conversion efficiency[2]. Beyond their performance, perovskites are the subject of intense research interest due to their

Sustainable Energy & Fuels Accepted Manuscript

View Article Online
DOI: 10.1039/C7SE00545H

Published on 12 February 2018. Downloaded on 12/02/2018 15:37:05.

potential for easier and lower-cost manufacturing than the market-leading silicon solar technology. However, ensuring the long-term stability of perovskite solar cells remains a challenge for commercialization of this technology. Perovskite solar cells tend to degrade prematurely depending on the films quality and atmospheric conditions. Humidity[3,4,5], light[6], oxygen[7], temperature[8] and more recently electrical stress[9,10] have been shown to play an important role in initiating degradation pathways. Among these, electrical stress in "dark" has been very rarely investigated despite being a critical parameter for solar cells. Besides, perovskites are also being considered for other optoelectronic devices such as field-effect light emitting diodes (LEDs)[11], transistors[12] or lasers[13], which also operate under an external bias. In particular, LEDs have an architecture and films thickness similar to solar devices but a relatively high turn-on voltage of 3-4 V. This implies that perovskites should be stable under high electric field to achieve maximum external quantum efficiency and luminance[14,15].

Various mechanisms have been proposed to explain the degradation of the perovskite phase and resulting device performance upon applying an electric field in the dark. Using a laterally contacted device, it was suggested that methylammonium cations are loosely bound in the hydrated perovskite phase formed in the presence of moisture[10]. These cations drift and accumulate near the negative electrode under the effect of an electric field, which leads to the irreversible structural modification of the depleted perovskite into PbI_2 near the positive electrode. Ions migration was also observed by temperature-dependent dark current decay in a standard (top-anode) perovskite device architecture[9]. The device stability was found to strongly depend on the level of applied voltage in the dark. Irreversible degradation was observed when $V_{applied} > V_{oc}$. This was explained by the inversion of the space charge region at the electron transport layer (ETL) interface after the displacement of a high density of ionic defects (ions or

Sustainable Energy & Fuels Accepted Manuscript

View Article Online
DOI: 10.1039/C7SE00545H

ion vacancies). Unlike these observations, D. Bryant and co-workers showed that the rapid electrical bias-induced degradation of $CH_3NH_3PbI_3$ in a standard device architecture can be attributed to the diffusion of oxygen in the perovskite lattice and formation of highly reactive superoxide species O_2^- when electrons are not extracted efficiently from the active layer[16]. In this case, slower degradation was observed when devices were exposed to moisture alone. Hence a crucial question is to ascertain which mechanism is responsible for the degradation of PSCs under applied bias in "dark" and to clearly establish the role played by superoxides or/and ionic defects migration.

In this work, we prepared inverted PSCs using NiO_x as HTL and investigated the effect of electrical bias in "dark" on the device performances and material properties. NiO_x hole transport layer was chosen in this study because of its higher efficiency and reproducibility over more commonly used PEDOT:PSS. Moreover, in the course of this study, we also investigated typical PEDOT:PSS and organic small molecules as alternative HTLs and observed similar degradation, which tend to show that the degradation can be quite general. To the best of our knowledge, study on the bias degradation of inverted PSCs in dark is "missing" although they have several advantages over standard top-anode devices such as less hysteresis and lower processing temperatures, while record efficiencies are getting comparable to the standard architecture. Besides, important questions remain for the dark bias degradation such as: What is the chemical origin of such degradation? How does the device degrade structurally? Here, we provide some insights to these questions together with new and advanced structural probes.

Methods

1.1 Materials

Published on 12 February 2018. Downloaded on 12/02/2018 15:37:05.
Sustainable Energy & Fuels Accepted Manuscript

View Article Online
DOI: 10.1039/C7SE00545H

Published on 12 February 2018. Downloaded on 12/02/2018 15:37:05.

All materials were used without purification. Anhydrous dimethyl sulfoxide (DMSO), *N,N*-dimethylformamide (DMF), anhydrous ethanol, anhydrous chlorobenzene, anhydrous ethanolamine, anhydrous 2-methoxyethanol, bathocuproine (BCP, 96%), nickel acetate (Ni-acc, 98%) and lead iodide (PbI_2, 99%) were purchased from Sigma-Aldrich. Methylammonium iodide (MAI) was purchased from Dyesol. The electron transport material [6,6]-phenyl-C_{61} butyric acid methyl ester (PCBM) was obtained from Solenne BV. To prepare the NiO_x solution, 0.2 M solution of nickel acetate tetrahydrate was dissolved in a 1:0.012 volume ratio of 2-methoxyethanol:ethanolamine and stirred for 1 h at 60°C. $CH_3NH_3PbI_3$ precursor solution was prepared by mixing CH_3NH_3I and PbI_2 (1:1.05 molar ratio) in DMF/DMSO (4:1 volume ratio) with a concentration of 804 mg mL^{-1} at 60°C for 2 h. PCBM was dissolved in chlorobenzene with concentration 20 $mg.ml^{-1}$ and stirred overnight at 60°C. BCP was dissolved in anhydrous ethanol with concentration 0.5 $mg.ml^{-1}$. All solutions were filtered with 0.45 μm PTFE syringe filters.

1.2 Perovskite solar cell fabrication and testing

15 $\Omega.\square^{-1}$ ITO/glass substrates (Lumtec) were sequentially cleaned with detergent in DI water, acetone, and isopropyl alcohol in an ultrasonic bath. Subsequently, they were dried with N_2 and exposed to O_2 plasma for 10 min. □20 nm-thick NiO_x layer was deposited via spin-coating at 4000 rpm for 30 s followed by 30 min sintering at 250°C. Subsequent layers were prepared under nitrogen in a glove box. The perovskite precursor solution was spin coated at 4000 rpm for 30 s. Chlorobenzene was drop-cast onto the rotating sample after 15 s of spinning to promote crystallization. The 400 nm perovskite film was annealed at 100°C for 10 min. After cooling, the PCBM solution was spin-coated onto the $CH_3NH_3PbI_3$ layer at 4000 rpm for 30 s, followed by spin-coating the BCP solution at 6000 rpm for 20 s. The thickness of the PCBM is □60 nm. The

Sustainable Energy & Fuels Accepted Manuscript

View Article Online
DOI: 10.1039/C7SE00545H

thickness of the BCP film is too thin to be measured by profilometry or SEM. Finally, 100 nm thick silver counter electrodes were evaporated at 10^{-4} Torr using an Edwards 306 thermal evaporator, forming devices with an active area of 0.15 cm^2.

Current density–voltage (J–V) characterizations were performed by a Keithley 2400 source-meter unit under 0.8 sun illumination using a Newport 92193A-1000 solar simulator. Current-voltage sweeps were performed from both V_{OC}-to-J_{SC} and vice versa at a rate of 0.1 V s^{-1}.

1.3 Material characterizations

The Raman and photoluminescence measurements were performed with a Renishaw Invia Raman system in backscattering configuration. A 532 nm laser and 50x objective were used (NA: 0.50, spot size ≈ 1 μm). For single point Raman measurements, a laser power of 0.6 mW and acquisition time of 30 s were used; For the Raman and PL line mapping, 0.6 mW/5 s and 0.06 μW/1 s laser power/acquisition time were used for each measurement point, respectively. 1800 gr/mm and 300 gr/mm gratings were used for Raman and photoluminescence, respectively. Local photocurrent measurements were acquired using the laser beam and X-Y scanning stage from the Raman system (Renishaw Invia, 532 nm, 50x objective) and a source-meter unit Keithley 236. The devices were contacted using a Linkam atmospheric chamber. The solar cell was held at short-circuit in the dark until the residual current dropped below 5 nA (which can take up to 60 s). Then, the laser shutter was open and the photocurrent was monitored over time. A low laser power of 0.3 mW was used to avoid any further degradation of the perovskite film by the laser beam during the measurement.

Published on 12 February 2018. Downloaded on 12/02/2018 15:37:05.
Sustainable Energy & Fuels Accepted Manuscript

View Article Online
DOI: 10.1039/C7SE00545H

XRD measurements were carried out using a Bruker D8 Discover instrument with a CuKα beam (wavelength is 0.15418 nm) at 40 kV and 40 mA, scan parameters of 1 s/step at 0.03° of 2θ step size.

The basic principles of the experimental method to collect hyperspectral images (SEHI) have been reported by P. Kazemian et al.[17] In this work, we used FEI Helios NanoLab G3 UC SEM. All the samples are imaged using through-lens detector (TLD) at a working distance of 4.0 mm with a beam current of 6.3 pA and an accelerating voltage of 1 kV. The required hyperspectral window was selected (0-6.0 eV) by setting the mirror electrode to 0 V. For all SEHI images, the dwell time was adjusted to 50 ns.

Chronoamperometry measurements were carried out using a Keithley 236 source-meter unit controlled by software. The dark current through the cell was continuously recorded during the applied voltage sequence: the cell was first left at short-circuit for 30 s to allow equilibrium to be reached. Then, a forward bias of 1 V was applied for 30 s before the device was switched to short-circuit mode (0 V) for 30 s (until the current stabilized to a few nanoamperes). The device was switched on and off successively several times. The same procedure was also carried out at 0.5 V and 0.85 V.

The total charge density was estimated from the current transients at short-circuit condition by integrating the current decay as described below:

$$Q = \frac{1}{A \times d} \int \frac{I(t)}{e} dt \qquad (1)$$

Where Q is the charge density, A the surface of the electrode, d the thickness of the perovskite layer, e the electronic charge and I the current at short circuit conditions.

Published on 12 February 2018. Downloaded on 12/02/2018 15:37:05.

Sustainable Energy & Fuels Accepted Manuscript

View Article Online
DOI: 10.1039/C7SE00545H

Published on 12 February 2018. Downloaded on 12/02/2018 15:37:05.

Results and Discussion

We first investigated the effect of electrical bias in dark coupled with water vapor and/or oxygen on the PSCs performance. PSCs with structure glass/ITO/NiO_x/$CH_3NH_3PbI_3$(MAPI)/$PC_{60}BM$/BCP/Ag were fabricated and subjected to 1 V forward bias in air (40% RH), dry N_2, dry air and humid N_2. All degradations in this work were performed in the dark. In the case of humid N_2, a water-saturated atmosphere (≈100% humidity) was obtained by flowing N_2 through a sealed water jar. The current-voltage (J-V) curves before and after bias applications are shown in Figure 1a. When exposed to air or humid N_2, the cell drastically degraded after 1 h bias application mostly due to a large drop in J_{sc}. When exposed to dry N_2 or dry air, the biased cells only suffered minor degradation characterized by a slight drop of the J_{sc}, but no change in FF or V_{oc}. These results demonstrate the key role played by water vapor in the degradation of PSCs under bias in the dark, whereas oxygen does not have a significant effect. Even in scenarios where devices were degraded in dry N_2 or dry air, the slight loss in efficiency (from 10.4% to 8.8% and 10.7% to 8.8%, respectively) may be attributed to the presence of small amounts of water (or any polar molecules as explained by Leijtens *et al.*[10]) in the perovskite stack, due to the sample being exposed to the ambient atmosphere prior to conducting the degradation tests, or perhaps while in contact with polar solvents in the glovebox during device fabrication. Oxygen and the formation of superoxides, although suggested by others[16] as another important path towards the degradation of lead halide perovskite materials, doesn't appear to have a significant effect in this case (dark, dry environment, 1 V). It was shown that oxygen molecules enter the perovskite at a fast rate and uniformly saturate perovskite vacancies after a few seconds only[18]. As we purged the atmospheric chamber for 10 min before measurement with a relatively high flow rate of dry air, it is reasonable to assume that samples

Sustainable Energy & Fuels Accepted Manuscript

View Article Online
DOI: 10.1039/C7SE00545H

Published on 12 February 2018. Downloaded on 12/02/2018 15:37:05.

exposed to this environment were saturated with oxygen when the bias was applied. The fact that the device was relatively stable under dry air (same trend as in dry N_2) diminishes the role of highly reactive superoxide species, at least during the first hour of degradation.

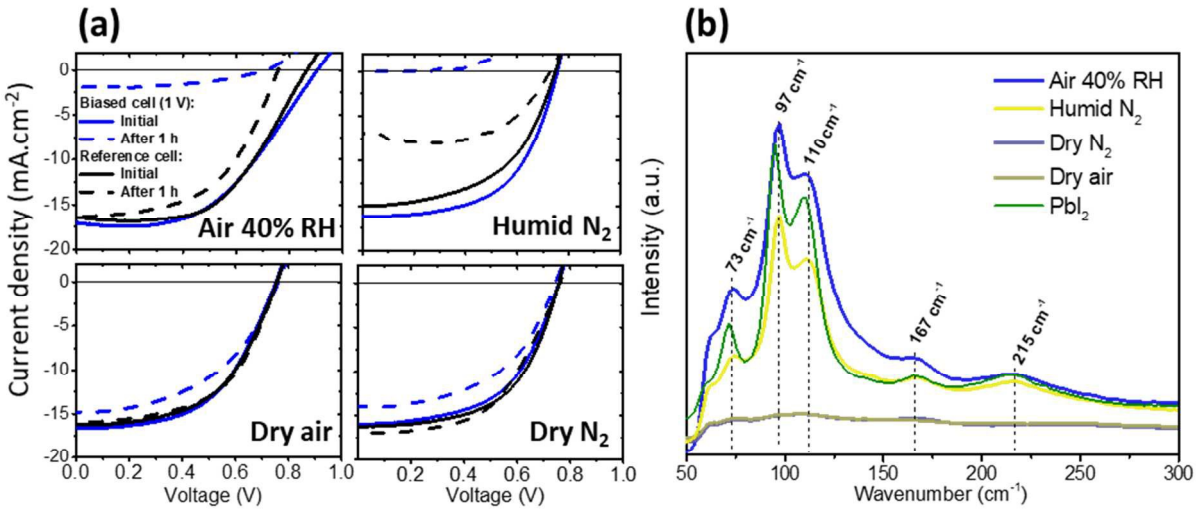

Figure 1. (a) Current density – voltage curves of perovskite devices at 0.8 sun before (solid blue lines) and after (dashed blue lines) biasing at 1 V for 1 h under dark condition in different atmospheres. Reference cells left in the same environment for the same duration but without bias are also shown for comparison (black lines). (b) Corresponding Raman spectra for the biased cells and reference PbI_2 film (intensity divided by 10 times for comparison).

Figure 1b shows the Raman spectra for the four different cells after degradation. The cells degraded in 40% RH air and humid N_2 reveal the features of PbI_2, with a main peak at 97 cm^{-1} associated to the stretching mode of Pb-I[19] (the higher intensity measured for 40% RH is due to local inhomogeneities but does not reflect the degradation level), and other characteristic peaks at 75 cm^{-1}, 110 cm^{-1}, 167 cm^{-1} and 215 cm^{-1}. This indicates that a large fraction of the MAPI converted to PbI_2 when exposed to 40% RH air or humid N_2 under 1 V bias. In the case of

Sustainable Energy & Fuels Accepted Manuscript

View Article Online
DOI: 10.1039/C7SE00545H

devices exposed to dry air or dry N_2, the Raman data confirm very small amount of PbI_2, thus correlating device performance results.

Numerous reports showed that metal contacts play an important role in the degradation of perovskite devices. In particular, it has been observed that in presence of moisture, Ag can be converted to AgI due to the migration of I^- ions and Ag through pinholes in the Spiro-OMeTAD layer in the standard architecture[20]. However, we didn't observe any XRD diffraction peaks due to AgI (peaks at $2\theta = 22.3°$, 23.8°, and 39.2° for β-AgI)[21] when measuring the bias degraded cell (1 V, 1 h, humid N_2) through the Ag top electrode (Figure S1a, blue curve). It suggests that such degradation mechanism is not likely to happen in the inverted perovskite device structure, and can be explained by the fundamental difference that unlike standard device structure, a positive bias is applied to the ITO and not to the Ag electrode for the inverted device structure (so negative ions will be attracted to the ITO).The only difference between the XRD spectra of the degraded and non-degraded cell is the appearance of PbI_2 peak at 12.6° after degradation, which agrees well with the Raman results.

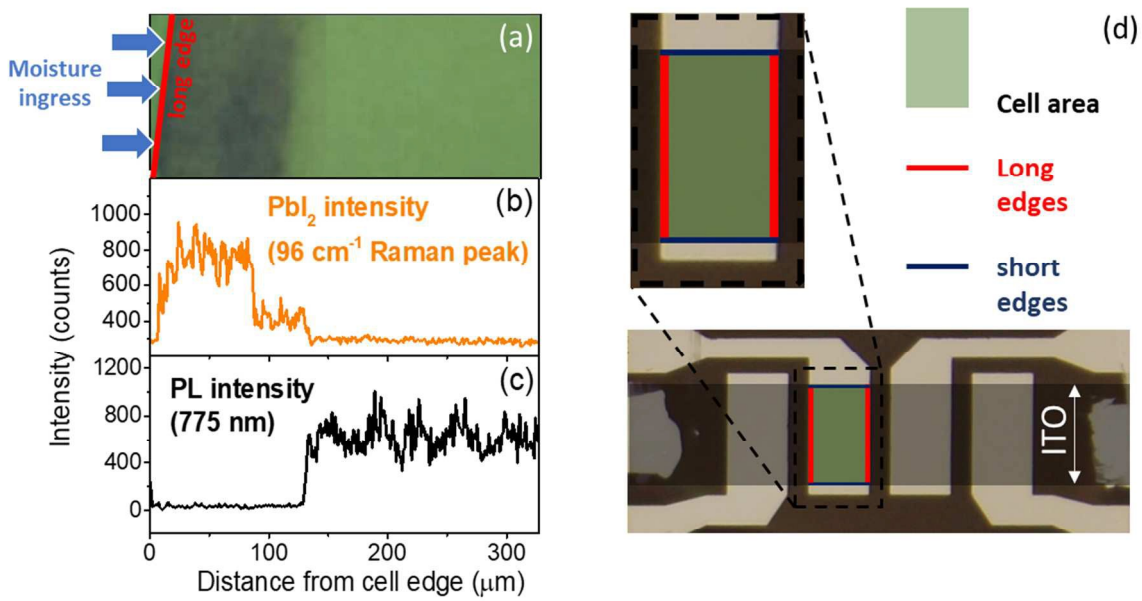

Published on 12 February 2018. Downloaded on 12/02/2018 15:37:05.
Sustainable Energy & Fuels Accepted Manuscript

View Article Online
DOI: 10.1039/C7SE00545H

Figure 2. (a) Optical microscope image of the "long" edge of the degraded perovskite cell after 20 min under 1 V bias in humid air. (b) PbI_2 Raman intensity profiles measured at 96 cm^{-1} along the edge. (c) Photoluminescence peak intensity profile at 775 nm. (d) Optical image showing the ITO and Ag electrodes delimitating the cells measured in this work. The "long" and "short" edges of the cells are shown as red and blue lines, respectively.

To confirm the role of moisture in the degradation of PSCs, freshly prepared samples were exposed to humid N_2 environment for 20 min without bias. This procedure allowed water molecules to penetrate within the perovskite film, in particular where the stack is not covered by the Ag top electrode or near the edges of the electrode. After this preconditioning, a bias was applied in air for short times, and optical microscopic images of the cell edge were recorded at different intervals (Figure S2). No visual degradation is observed up to 70 s at 1 V bias, before exposure to humid N_2. However, following exposure to humidity, the application of a bias clearly triggers the appearance of degradation features after a few seconds only. These are particularly concentrated near the long edge of the cell while the center of the cell and short edges are much better preserved. In this paper, the "long" edges are defined by the silver top electrode, while the "short" edges are defined by the ITO stripe, as shown in Figure 2(d). Similar patterns were observed when the cell is exposed to air with 40% RH and biased for 20 min, as shown in Figure 2a. These observations were further correlated with Raman and photoluminescence intensity profiles acquired across 300 μm from outside the edge of a cell toward the center, as shown in Figure 2b and c. The results show that the cell is highly degraded across 130 μm, starting from the edge of the cell. This is supported by 3-fold increase of PbI_2 Raman peak at 96 cm^{-1} and more than 10 times drop in PL intensity at 775 nm.

Published on 12 February 2018. Downloaded on 12/02/2018 15:37:05.

Sustainable Energy & Fuels Accepted Manuscript

View Article Online
DOI: 10.1039/C7SE00545H

Published on 12 February 2018. Downloaded on 12/02/2018 15:37:05.

The degradation pattern could be explained as follows: the 100 nm-thick silver top electrode acts as a barrier for water vapor and protects, to some extent, the underlying perovskite film. However, moisture ingress is much stronger at the long edges of the cell where the silver electrode finishes. As water penetrates in the device stack from the long edge of the cell, hydrated phases of perovskite are formed (as shown by several reports[3,4,22]), which then rapidly converts to PbI_2 under the effect of the electric field (Figure S1). In comparison, when the cell was not previously hydrated, the bias-induced degradation happens in minutes instead of seconds because of the much lower density of water molecules presents in the MAPI film (Figure 2). We also observed that the short edges were much less degraded than the long edges. Indeed, the short edges are delimitated by the ITO bottom electrode while the Ag electrode continues further away, thus better protecting the short edges from environmental conditions.

XRD measurements were also carried out to investigate the formation of hydrated phases of perovskite when exposed to a humid environment. For this purpose, a sample was measured by focusing the X-ray beam outside the Ag electrode, to directly probe the perovskite/PCBM/BCP film after exposure to high humidity environment (1 h, 100% RH in N_2). For repeated measurements on different samples, most of the time no diffraction peaks due to monohydrate $CH_3NH_3PbI_3{:}H_2O$ or dihydrate $(CH_3NH_3)_4PbI_6{:}2H_2O$ were observed.[3] However, these metastable intermediate phases are usually difficult to measure because they are time and space-limited. Even recent in-situ synchrotron XRD measurements in high humidity environment could detect hydrated phases only from time to time during the degradation process.[22] Thus, the fact that we couldn't easily detect such phase doesn't mean that monohydrate or dihydrate perovskite is not formed when moisture penetrates within the film, especially as the samples were measured at least 15 min after high humidity exposure and could have dried in the meantime depending on

Sustainable Energy & Fuels Accepted Manuscript

View Article Online
DOI: 10.1039/C7SE00545H

Published on 12 February 2018. Downloaded on 12/02/2018 15:37:05.

1 the atmospheric conditions (Leguy et al. showed that hydrated perovskite crystals can dry in less
2 than 15 min when exposed to dry air)[3]. Note that, occasionally, we observed a new peak at 37.9°,
3 which has similar position to the XRD peak of $(CH_3NH_3)_4PbI_6{:}2H_2O$ (Figure S1b, orange
4 curve)[3]. It tends to suggest that hydrated perovskite phases form in the film, although they are
5 momentary and dependent on the atmospheric conditions.

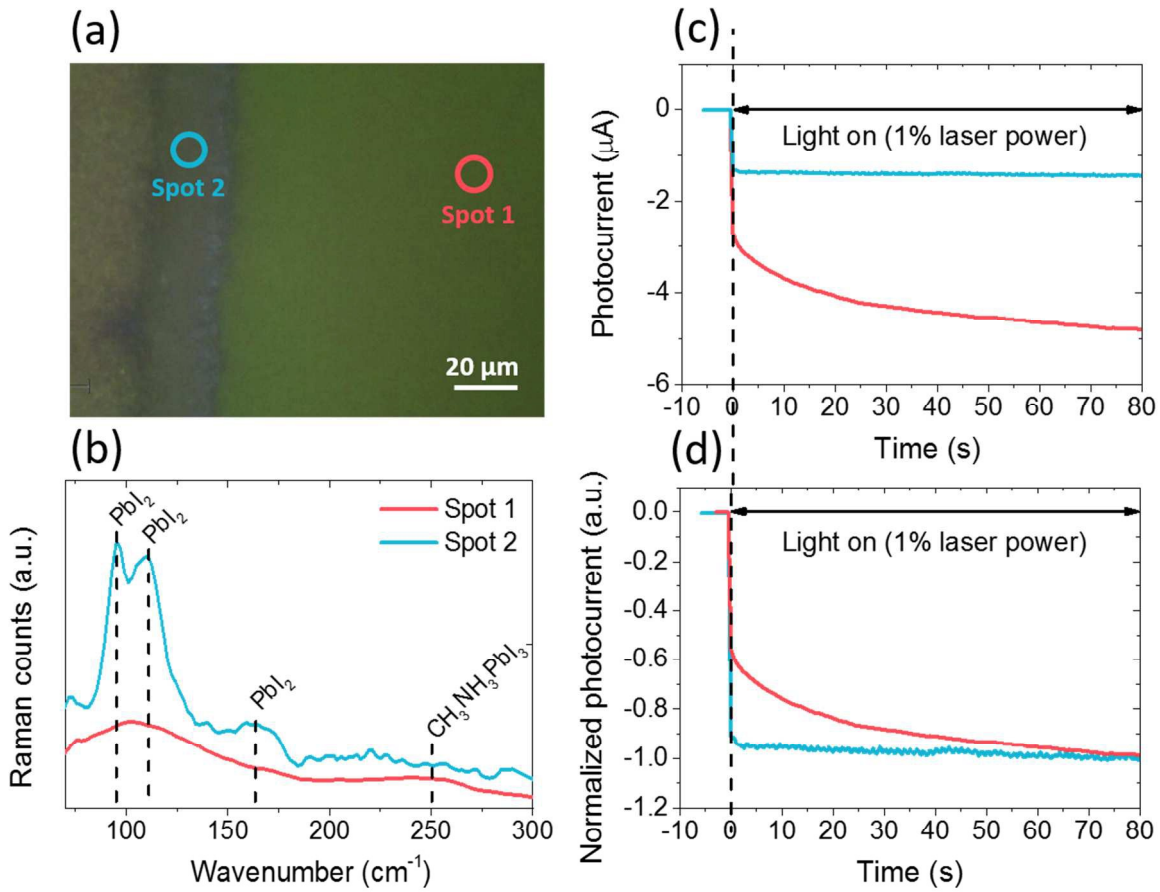

6

7 **Figure 3.** (a) Optical microscope image of the degraded cell with the 2 different regions (edge
8 and inner side of the cell) used for local characterizations (b –d). (b) Micro-Raman spectra. (c)
9 Local photocurrent stabilization curves measured at short-circuit (laser excitation power □0.3
10 mW). (d) Normalized photocurrent stabilization curves.

Sustainable Energy & Fuels Accepted Manuscript

View Article Online
DOI: 10.1039/C7SE00545H

Published on 12 February 2018. Downloaded on 12/02/2018 15:37:05.

At this stage, the results demonstrate that the combined effects of water molecules ingress and applied bias are responsible for the degradation of the perovskite film to PbI_2. Next, making use of the various degradation levels that are formed at the cell edge after biasing, we performed localized photoelectrical characterizations by focusing the laser beam of the Raman system (□1 μm diameter) at the center (region 1) or at the edge (region 2) of the cell, as represented in Figure 3a. The Raman spectra shown in Figure 3b confirm that two distinct levels of degradation are obtained: for region 1, the $CH_3NH_3PbI_3$ phase was well preserved, showing two broad peaks at 250 cm^{-1} and 110 cm^{-1}, which can be assigned to the methylammonium cations torsional and libration modes, respectively[23]. For region 2, significantly more PbI_2 (at 96 cm^{-1} and 110 cm^{-1}) relative to $CH_3NH_3PbI_3$ is generated. Although a clear Raman signal from $CH_3NH_3PbI_3$ at 250 cm^{-1} was not observed for region 2, it does not necessary mean that all perovskite degraded to form PbI_2, as the Raman cross-section of perovskite is much lower than that of PbI_2 and thus can be masked by the much stronger PbI_2 signal[19]. This is further supported by the significant amount of photocurrent generated at region 2 although PbI_2 absorbs very little (if any) at the laser excitation wavelength, as explained in the next paragraph.

Photocurrent stabilization curves for the two different regions are shown in Figure 3c and d. To ensure that all measurements were started from the same equilibrium condition, the solar cell was held at short-circuit in the dark until the residual current dropped below 5 nA (which can take up to 60 s). Then, the laser shutter was opened and the photocurrent was monitored over time. A low laser power of 0.3 mW was used to avoid any further degradation of the perovskite film by the laser beam during the measurement[19]. On the non-degraded region (region 1), the photocurrent quickly switches to -2.7 μA but then gradually rises to reach -4.8 μA after 80 s. On the contrary, for the highly degraded region (region 2), the photocurrent quickly reaches a

Sustainable Energy & Fuels Accepted Manuscript

View Article Online
DOI: 10.1039/C7SE00545H

Published on 12 February 2018. Downloaded on 12/02/2018 15:37:05.

stabilized value of -1.4 μA without long transients. The long photocurrent transient can be explained by ion migration according to several recent works[24,9,25]. The photovoltage induces mobile ions to slowly move in the perovskite layer and to screen the electric field until ions reach a new equilibrium. This slow motion of mobile ions (and vacancies) is observed by the rise of the photocurrent toward a steady-state value at short-circuit on turning on the illumination. Alternatively, Shao et al. explained the slow photocurrent transient by trap filling process at grain boundaries and perovskite surface[26].

The results shown in Figure 3(b) and (d) indicate that when a large amount of PbI_2 is formed, the photocurrent transient is suppressed: the photocurrent quickly switches to a stabilized value, similarly to crystalline silicon solar cells which don't have ionic conductivity[9]. The two different rising times for the photocurrent measured on regions 1 and 2 are more clearly observed on the normalized curves in Figure 3d. Since PbI_2 has very low absorption at 532 nm[19], it is likely that the photocurrent measured on region 2 is generated in residual perovskite which was masked in the Raman spectra by the large amount of PbI_2 formed. These results are in good agreement with recent reports showing that incorporating some excess PbI_2 into $CH_3NH_3PbI_3$ solution[27] or forming PbI_2 secondary phase in $CH_3NH_3PbI_3$ film through post-deposition thermal annealing[25] can significantly reduce J-V hysteresis by suppressing ion migration. Obviously, the amount of PbI_2 formed at the edge of the cell is much too high to improve the device performance in our case but the results indicate that ion migration can be suppressed or highly reduced in the residual perovskite as a large amount of PbI_2 is formed. Hence, the local Raman-photoelectrical characterizations of perovskite solar cells give direct physical insights on the correlation between the local degradation (amount of PbI_2) and local electronic-ionic processes with micrometer

Sustainable Energy & Fuels Accepted Manuscript

View Article Online
DOI: 10.1039/C7SE00545H

resolution. To our knowledge, the information obtained by this novel technique cannot be obtained by other approaches.

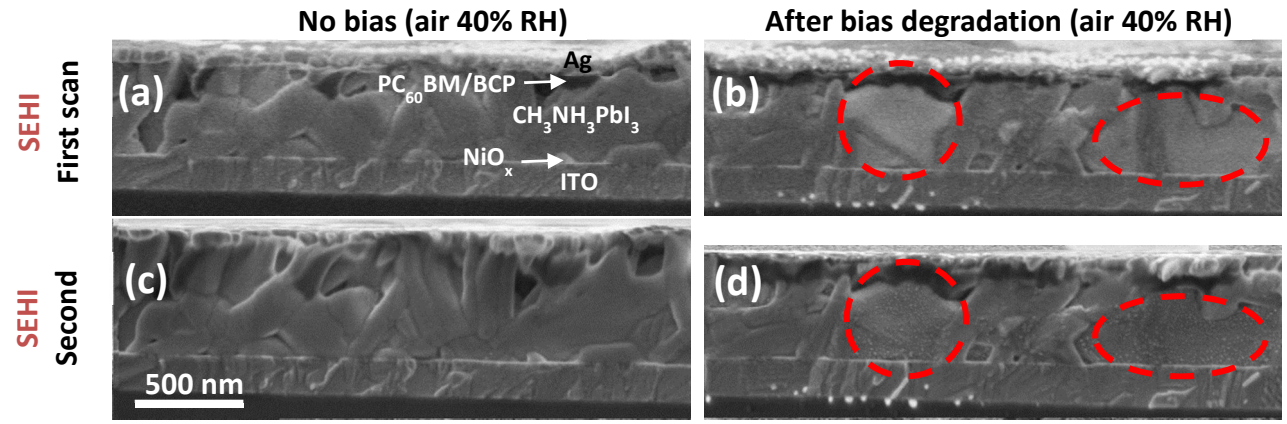

Figure 4. Cross-sectional hyperspectral secondary electron images (SEHI) in the range 0-6.0 eV before (a) and after (b) bias-induced degradation in 40% RH air (1 V for 1 h). (c) and (d) SEHI of the same devices and areas after a second scan.

Next, to better understand the effect of applied bias on the degradation of the perovskite layer in the presence of moisture, secondary electron hyperspectral cross-sectional images were acquired on a cell biased at 1 V in 40% RH air for 1 h, and compared to those of a reference cell (no bias). Secondary electron hyperspectral imaging (SEHI) is an advanced imaging technique making use of differences in the secondary electrons spectra of materials in a SEM to characterize local variations in the composition and electronic structure of materials with sub-10 nm resolution[28]. The hyperspectral images in Figure 4 show uniform contrast across the reference sample (Figure 4a), but clear contrast variations in the case of the degraded sample: some grains appear brighter than others (Figure 4b). It suggests a modification of the chemical composition of these grains, consistent with the hypothesis of ion migration. Interestingly, the contrast variation indicates that the degradation is not uniform at the sub-micrometer scale and varies when comparing individual

Published on 12 February 2018. Downloaded on 12/02/2018 15:37:05.
Sustainable Energy & Fuels Accepted Manuscript

View Article Online
DOI: 10.1039/C7SE00545H

Published on 12 February 2018. Downloaded on 12/02/2018 15:37:05.

grains. We suggest that the degradation ability of each crystalline grain under bias depends on the initial structural quality and composition of the grain. Indeed, the concentration of mobile defects in individual grains can be affected by the processing conditions which often lead to local non-uniformity[29]. Here, based on the clear contrast variations observed between crystalline grains from the same perovskite film, we may conclude that the application of an electrical bias is responsible for the drift of variable concentrations of ionic defects within each grain, resulting in distinct levels of highly localized degradation. At this stage of development of the technique (SEHI), it is not possible to measure the precise composition of the degraded grains. However, the Raman (and XRD) results suggest that these grains are composed of a large amount of PbI_2. The fact that both degraded and non-degraded grains sit next to each other at the microscopic scale in the highly degraded perovskite confirms that residual non-degraded perovskite remains in the degraded cell, which correlates well with the local photoelectrical characterizations (Figure 3c and d).

Further evidence of the localized level of degradation of individual grains is provided by comparing Figure 4b and 4d, illustrating two consecutive secondary electron hyperspectral images of the same cross-section area of the biased sample in the energy range 0-6 eV (additional images provided in SI Figure S3). In Figure 4d, 20-30 nm size dots were found to appear at the surface of bright degraded grains (red circles, magnified image in Figure S4), but not at the surface of darker grains. This is in agreement with other works showing that even moderate e-beam currents (86 pA) and acceleration voltages (10 kV) can induce an aggressive and very localized degradation of perovskite films due to ion migration[30,31]. In comparison, the reference sample did not show the appearance of e-beam induced-nano scale dots (Figure 4c). These results confirm that the composition of some specific crystalline grains was modified by

Sustainable Energy & Fuels Accepted Manuscript

View Article Online
DOI: 10.1039/C7SE00545H

biasing the device in humid air, and thus became even more sensitive to further degradation by the e-beam. We note that SEHI could be a fast and efficient novel method to investigate the chemical changes due to degradation in individual grains inside the film, which is particularly interesting for PSCs.

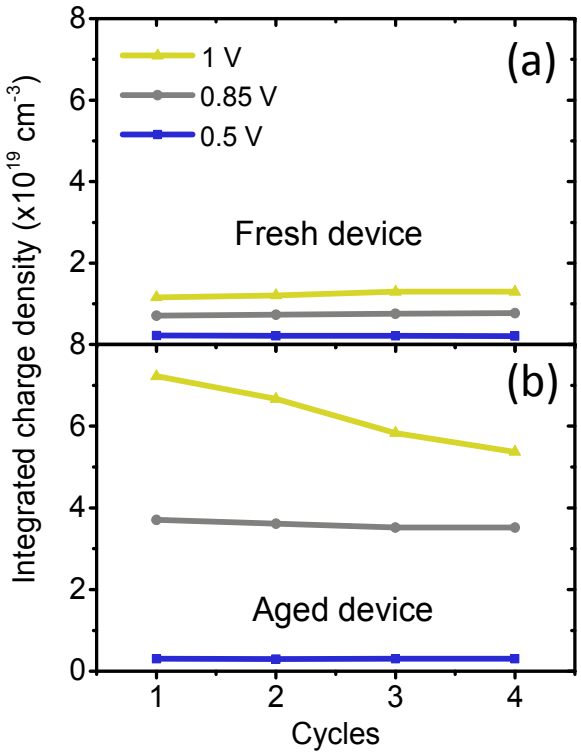

Figure 5. Integrated charge density (proportional to mobile ionic defects density) estimated from the integration of the transient part of the dark current at short-circuit condition just after biasing at 0.5 V, 0.85 V and 1 V for (a) a fresh perovskite device and (b) a device aged in air for two days.

To further understand the complementary roles of ion migration and humidity in the bias-induced degradation of perovskite devices, solid-state stepped chronoamperometry measurements were carried out. At this stage, the question is: can we correlate the degradation of

Published on 12 February 2018. Downloaded on 12/02/2018 15:37:05.
Sustainable Energy & Fuels Accepted Manuscript

View Article Online
DOI: 10.1039/C7SE00545H

the device performance under electrical bias with the density of mobile ionic defects in the perovskite, and how is it related to the presence of moisture?

In Figure S5, dark current measurements for square wave voltage with various peak voltages show the "discharging" behavior below V_{oc} and "charging" behavior above V_{oc} until steady-state is reached after a few seconds. These transient behaviors have been previously explained by the movement of ions in the perovskite layer which screen the electric field for seconds as the dynamics response of ions is much slower than electrons and holes[32,9]. If other mechanisms than ion migration may affect the current response, such as ferroelectric polarization or trapping of electrons at the interfaces, the rate of these mechanisms would be likely to be fast[33,34] relative to the slow timescales of current response shown in Figure S5.

The transient response of the dark current to a potential step has been used to estimate the density of mobile ions present in perovskite devices. In Figure S6, square wave potential steps between 0 and 1 V were applied on the device while the dark current was monitored. The shape of the dark current curve can be explained similarly to transistor-type device used by D. Li *et al.*[35]: when a positive bias (1 V) is applied on the device, a current is immediately measured due to the drift of electronic carriers in the device. The bias then induces mobile ions to gradually move toward the contacts until equilibrium is reached after a few seconds when the ion-induced electric field cancels the applied bias in the perovskite bulk, which is observed by the stabilization of the dark current. After removing the applied bias (0 V), the previously accumulated ions at the perovskite−electrode interfaces create a net reversal electric field, leading to an instant switching of the polarity of the electronic current. The accumulated ions gradually diffuse away from the perovskite−electrode interfaces, resulting in the decrease of the ion-induced electric field and thus the reduction of the dark electronic current. If it is quite clear

Published on 12 February 2018. Downloaded on 12/02/2018 15:37:05.
Sustainable Energy & Fuels Accepted Manuscript

View Article Online
DOI: 10.1039/C7SE00545H

that there is interplay between the ionic and electronic current, it may be asked the origin of electronic carriers in the dark. It can be explained by the build-up of an electrostatic potential at the interfaces due to the band bending induced by ions accumulation, as explained by R. Gottesman et al.[36]. When the bias is switched off, the electrostatic potential at the interface remains for a few seconds before the device is "discharged" when mobile ions reached a new equilibrium.

From this picture, we see that the magnitude of the ion-induced electric potential (or amount of displaced mobile ions) will affect the magnitude and time constant of the measured dark current. By integrating the area below the electronic current decay, we can thus estimate an "integrated charge density" which is proportional to the amount of ions displaced in the device (mobile ions density). This measurement is similar to a recent work by S. Bae et al.[9] except that the dark current is integrated after the voltage is removed.

Two cells from the same sample were measured shortly after fabrication and after storage in air (40% RH) for two days (Figure 5). For the fresh cell, the integrated charge density is 2 x 10^{18} cm^{-3} at 0.5 V bias and increases up to 1.2 x 10^{19} cm^{-3} at 1 V. For the aged cell, the charge density is similar at 0.5 V bias (3 x 10^{18} cm^{-3}) but considerably increases with higher voltage, up to 7.2 x 10^{19} cm^{-3} at 1 V, which is 6 times higher than the fresh cell. As the sample was exposed to air without encapsulation, environmental moisture entered within the perovskite film and likely formed a hydrated phase containing more loosely bond ions[10]. At 0.5 V forward bias, the electric field is too low to activate these ions, which remain fixed in the crystalline structure. Thus, similar charge density is measured for the fresh and aged cells. However, at 0.85 V or 1 V the electric field is then sufficient to activate loosely bond ions and allow them to migrate in the hydrated perovskite (aged cell), which explains the significant increase in charge density. These

Published on 12 February 2018. Downloaded on 12/02/2018 15:37:05.
Sustainable Energy & Fuels Accepted Manuscript

View Article Online
DOI: 10.1039/C7SE00545H

results can be correlated with the degradation of the performance of the fresh and aged cells under dark bias. In Figure S7b, it is observed that the fresh cell degrades in hours instead of minutes for the aged cell, meaning that the perovskite devices having higher density of mobile ionic defects degrade faster under applied bias.

In addition, for the aged cell it can be observed that the charges density is slowly decreasing from 7.2 x 10^{18} cm^{-3} after the first potential step at 1 V to 5.4 x 10^{18} cm^{-3} after 4 potential steps. This trend can be explained as follow[9]: as mobile ions move to the opposite interface under the effect of an electrical bias, they may be trapped if the space charge region at this interface is inverted, which happens if the applied voltage is greater than V_{oc} or if a large amount of ions is displaced. As these ions are trapped, they cannot flow back in the perovskite bulk when the cell is switched back to short-circuit and do not participate in the measured current decay, which explains the charge density decrease at 1 V observed for the aged cell. This is not true for the fresh cell which has a higher V_{oc} □ 1 V (current-voltage curves under 1 sun for the fresh and aged cells are shown in Figure S7a), i.e. similar to the applied bias, and lower charge density. In this case, the opposite interface is depleted but not inverted and mobile ions are less likely to be trapped. Indeed, the charge density remains unchanged even after four potential steps at 1 V.

Finally, the electrical bias stability of triple-cation mixed-halide perovskites was examined as they are known to have better moisture stability than conventional methylammonium lead halide perovskite[37,38]. For this purpose, $Cs_{0.1}(MA_{0.17}FA_{0.83})_{0.9}Pb(I_{0.83}Br_{0.17})_3$ perovskite solution was prepared following a recipe described in another work[39] and used as absorber layer in devices with the same architecture and interlayers as described above. The final device gave a maximum efficiency of 11.6%, which is closed to state-of-the-art performance for triple-cation perovskite processed on top of NiO_x[40]. Then, the dark bias stability of the device was measured by applying

Published on 12 February 2018. Downloaded on 12/02/2018 15:37:05.
Sustainable Energy & Fuels Accepted Manuscript

View Article Online
DOI: 10.1039/C7SE00545H

1 V forward bias for 1 h in 40% RH air. The J-V curves before and after aging are shown in Figure S9 and compared to a reference cell (without bias). The performances of the biased and non-biased cells are similar after aging, which indicates that the electrical bias has little or no effect on degradation for this kind of cells. This is ascribed to the better stability of $Cs_{0.1}(MA_{0.17}FA_{0.83})_{0.9}Pb(I_{0.83}Br_{0.17})_3$ perovskite to moisture. By avoiding the formation of a hydrated phase when exposed to moisture, the triple-cation mixed-halide perovskite device is unsensitive to the applied bias, which is on the contrary to $CH_3NH_3PbI_3$ cells which suffer from strong degradation when using the same aging conditions (Figure 1(a)). This is consistent with previous results showing that moisture can enhance ionic mobility in $CH_3NH_3PbI_3$, which will eventually have a detrimental and irreversible effect on the stability of the cells when an external bias is applied. Multiple-cation mixed-halide perovskites could be an efficient alternative for improving moisture and electrical bias stability of perovskite solar cells.

Conclusions

In summary, we showed that humidity is the main factor for the bias-induced degradation of inverted device based on $CH_3NH_3PbI_3$ perovskite in the dark, as degradation due to oxygen (superoxide) is not observed. Besides, XRD does not show any AgI, which implies that degradation related to Ag electrode is likely to be mild (if any), which is different to standard device structure, and can be explained by the fundamental difference that a positive bias is applied to the ITO in the inverted device structure (which attract I^- to the ITO side). Our results suggest that, as the perovskite solar cell is exposed to a humid environment, moisture penetrates in the film preferentially from the edges of the cell and likely forms a hydrated perovskite phase which contains a high density of loosely bond ions. Under the effect of an external electric field, mobile ionic defects drift in the perovskite, which results in the accelerated degradation of the

Published on 12 February 2018. Downloaded on 12/02/2018 15:37:05.
Sustainable Energy & Fuels Accepted Manuscript

View Article Online
DOI: 10.1039/C7SE00545H

active layer and eventually irreversible conversion of $CH_3NH_3PbI_3$ into PbI_2. Novel Raman – transient photoelectrical technique is developed which allows probing local photoelectrical properties on a highly degraded and non-degraded region. It indicates that the presence of a large amount of PbI_2 suppresses or strongly reduces the migration of ionic species in the residual perovskite. By applying advanced cross-sectional hyperspectral secondary electron imaging technique, inhomogeneous degradation of distinct crystal grains was observed at the nano-scale which could be explained by variations in the structural quality and ionic defects density from grain to grain. Our study provides significant insight into the bias degradation of inverted perovskite solar cells in the dark. Importantly, the new techniques developed and applied here should be powerful to study the degradation of perovskite solar cells and other optoelectronic devices in general.

Conflicts of interest

There are no conflicts to declare.

ACKNOWLEDGMENT

The authors acknowledge funding from the EPSRC (grant no EP/M025020/1 & EP/N008065/1), Welsh Assembly Government funded Sêr Cymru Solar Project, the European Union's Horizon 2020 research and innovation programme under the Marie Skłodowska-Curie grant agreement No 663830. They thank Dr. Joel Troughton and Dr. Trystan Watson for advice on device fabrication and Dr. Adam Pocket for discussions on device physics and ion migration.

Published on 12 February 2018. Downloaded on 12/02/2018 15:37:05.

Sustainable Energy & Fuels Accepted Manuscript

View Article Online
DOI: 10.1039/C7SE00545H

Published on 12 February 2018. Downloaded on 12/02/2018 15:37:05.

REFERENCES

(1) Kojima, A.; Teshima, K.; Shirai, Y.; Miyasaka, T. Organometal Halide Perovskites as Visible-Light Sensitizers for Photovoltaic Cells. *J. Am. Chem. Soc.* **2009**, *131* (17), 6050–6051.

(2) Yang, W. S.; Park, B.-W.; Jung, E. H.; Jeon, N. J.; Kim, Y. C.; Lee, D. U.; Shin, S. S.; Seo, J.; Kim, E. K.; Noh, J. H.; Seok, S. Il. Iodide Management in Formamidinium-Lead-Halide Based Perovskite Layers for Efficient Solar Cells. *Science (80-.).* **2017**, *356* (6345), 1376–1379.

(3) Leguy, M. A.; Hu, Y.; Campoy-quiles, M.; Alonso, M. I.; Weber, O. J.; Azarhoosh, P.; Schilfgaarde, M. Van; Weller, M. T.; Bein, T.; Nelson, J.; Docampo, P.; Barnes, P. R. F. Reversible Hydration of CH3NH3PbI3 in Films, Single Crystals, and Solar Cells. *Chem. Mater.* **2015**, *27*, 3397–3407.

(4) Yang, J.; Siempelkamp, B. D.; Liu, D.; Kelly, T. L. Investigation of CH3NH3PbI3 Degradation Rates and Mechanisms in Controlled Humidity Environments Using in Situ Techniques. *ACS Nano* **2015**, *9* (2), 1955–1963.

(5) Christians, J. A.; Miranda Herrera, P. A.; Kamat, P. V. Transformation of the Excited State and Photovoltaic Efficiency of CH3NH3PbI3 Perovskite upon Controlled Exposure

Sustainable Energy & Fuels Accepted Manuscript

View Article Online
DOI: 10.1039/C7SE00545H

Published on 12 February 2018. Downloaded on 12/02/2018 15:37:05.

to Humidified Air. *J. Am. Chem. Soc.* **2015**, *137* (4), 1530–1538.

(6) Leijtens, T.; Eperon, G. E.; Pathak, S.; Abate, A.; Lee, M. M.; Snaith, H. J. Overcoming Ultraviolet Light Instability of Sensitized TiO2 with Meso-Superstructured Organometal Tri-Halide Perovskite Solar Cells. *Nat. Commun.* **2013**, *4*, 2885.

(7) Pearson, A. J.; Eperon, G. E.; Hopkinson, P. E.; Habisreutinger, S. N.; Wang, J. T. W.; Snaith, H. J.; Greenham, N. C. Oxygen Degradation in Mesoporous Al2O3/CH3NH3PbI3-xClx Perovskite Solar Cells: Kinetics and Mechanisms. *Adv. Energy Mater.* **2016**, 1–10.

(8) Conings, B.; Drijkoningen, J.; Gauquelin, N.; Babayigit, A.; D'Haen, J.; D'Olieslaeger, L.; Ethirajan, A.; Verbeeck, J.; Manca, J.; Mosconi, E.; De Angelis, F.; Boyen, H. G. Intrinsic Thermal Instability of Methylammonium Lead Trihalide Perovskite. *Adv. Energy Mater.* **2015**, *5* (15), 1–8.

(9) Bae, S.; Kim, S.; Lee, S. W.; Cho, K. J.; Park, S.; Lee, S.; Kang, Y.; Lee, H. S.; Kim, D. Electric-Field-Induced Degradation of Methylammonium Lead Iodide Perovskite Solar Cells. *J. Phys. Chem. Lett.* **2016**, *7* (16), 3091–3096.

(10) Leijtens, T.; Hoke, E. T.; Grancini, G.; Slotcavage, D. J.; Eperon, G. E.; Ball, J. M.; De Bastiani, M.; Bowring, A. R.; Martino, N.; Wojciechowski, K.; McGehee, M. D.; Snaith, H. J.; Petrozza, A. Mapping Electric Field-Induced Switchable Poling and Structural Degradation in Hybrid Lead Halide Perovskite Thin Films. *Adv. Energy Mater.* **2015**, *5* (20), 1–11.

(11) Wang, N.; Cheng, L.; Ge, R.; Zhang, S.; Miao, Y.; Zou, W.; Yi, C.; Sun, Y.; Cao, Y.; Yang, R.; Wei, Y.; Guo, Q.; Ke, Y.; Yu, M.; Jin, Y.; Liu, Y.; Ding, Q.; Di, D.; Yang, L.; Xing, G.; Tian, H.; Jin, C.; Gao, F.; Friend, R. H.; Wang, J.; Huang, W. Perovskite Light-

Sustainable Energy & Fuels Accepted Manuscript

View Article Online
DOI: 10.1039/C7SE00545H

Emitting Diodes Based on Solution-Processed Self-Organized Multiple Quantum Wells. *Nat. Photonics* **2016**, *10* (11), 699–704.

(12) Yajima, T.; Hikita, Y.; Hwang, H. Y. A Heteroepitaxial Perovskite Metal-Base Transistor. *Nat. Mater.* **2011**, *10* (3), 198–201.

(13) Zhu, H.; Fu, Y.; Meng, F.; Wu, X.; Gong, Z.; Ding, Q.; Gustafsson, M. V.; Trinh, M. T.; Jin, S.; Zhu, X.-Y. Lead Halide Perovskite Nanowire Lasers with Low Lasing Thresholds and High Quality Factors. *Nat. Mater.* **2015**, *14* (6), 636–642.

(14) Zhao, L.; Gao, J.; Lin, Y. L.; Yeh, Y.-W.; Lee, K. M.; Yao, N.; Loo, Y.-L.; Rand, B. P. Electrical Stress Influences the Efficiency of CH3NH3PbI3 Perovskite Light Emitting Devices. *Adv. Mater.* **2017**, *1605317*, 1605317.

(15) Myoung, S.; Song, H. High-Performance Perovskite Light-Emitting Diodes via Morphological Control of Perovskite Film. *Nanoscale* **2016**, *8*, 7036–7042.

(16) Bryant, D.; Aristidou, N.; Pont, S.; Sanchez-Molina, I.; Chotchunangatchaval, T.; Wheeler, S.; Durrant, J. R.; Haque, S. A. Light and Oxygen Induced Degradation Limits the Operational Stability of Methylammonium Lead Triiodide Perovskite Solar Cells. *Energy Environ. Sci.* **2016**, *9*, 1655.

(17) Kazemian, P.; Mentink, S. A. M.; Rodenburg, C.; Humphreys, C. J. Quantitative Secondary Electron Energy Filtering in a Scanning Electron Microscope and Its Applications. *Ultramicroscopy* **2007**, *107* (2–3), 140–150.

(18) Aristidou, N.; Eames, C.; Sanchez-molina, I.; Bu, X.; Kosco, J.; Islam, M. S.; Haque, S. A. Fast Oxygen Diffusion and Iodide Defects Mediate Oxygen-Induced Degradation of Perovskite Solar Cells. *Nat. Commun.* **2017**, *8* (May), 1–10.

(19) Hooper, K. E. A.; Lee, H. K. H.; Newman, M. J.; Meroni, S.; Baker, J.; Watson, T. M.;

Published on 12 February 2018. Downloaded on 12/02/2018 15:37:05.

Sustainable Energy & Fuels Accepted Manuscript

View Article Online
DOI: 10.1039/C7SE00545H

Tsoi, W. C. Probing the Degradation and Homogeneity of Embedded Perovskite Semiconducting Layers in Photovoltaic Devices by Raman Spectroscopy. *Phys. Chem. Chem. Phys.* **2017**, *19*, 5246–5253.

(20) Zhang, T.; Meng, X.; Bai, Y.; Xiao, S.; Hu, C.; Yang, Y.; Chen, H.; Yang, S. Profiling the Organic Cation-Dependent Degradation of Organolead Halide Perovskite Solar Cells. *J. Mater. Chem. A* **2017**, *5* (3), 1103–1111.

(21) Kato, Y.; Ono, L. K.; Lee, M. V.; Wang, S.; Raga, S. R.; Qi, Y. Silver Iodide Formation in Methyl Ammonium Lead Iodide Perovskite Solar Cells with Silver Top Electrodes. *Adv. Mater. Interfaces* **2015**, *2* (13), 2–7.

(22) Zhao, J.; Cai, B.; Luo, Z.; Dong, Y.; Zhang, Y.; Xu, H.; Hong, B.; Yang, Y.; Li, L.; Zhang, W.; Gao, C. Investigation of the Hydrolysis of Perovskite Organometallic Halide CH3NH3PbI3 in Humidity Environment. *Sci. Rep.* **2016**, *6* (1), 21976.

(23) Quarti, C.; Grancini, G.; Mosconi, E.; Bruno, P.; Ball, J. M.; Lee, M. M.; Snaith, H. J.; Petrozza, A.; Angelis, F. De. The Raman Spectrum of the CH3NH3PbI3 Hybrid Perovskite: Interplay of Theory and Experiment. *J. Phys. Chem. Lett.* **2014**, *5*, 279–284.

(24) Eames, C.; Frost, J. M.; Barnes, P. R. F.; O'Regan, B. C.; Walsh, A.; Islam, M. S. Ionic Transport in Hybrid Lead Iodide Perovskite Solar Cells. *Nat. Commun.* **2015**, *6* (May), 7497.

(25) Du, T.; Burgess, C.; Kim, J.; Durrant, J.; Zhang, J.; McLachlan, M. Formation, Location and Beneficial Role of PbI2 in Lead Halide Perovskite Solar Cells. *Sustain. Energy Fuels* **2017**, 119–126.

(26) Shao, Y.; Xiao, Z.; Bi, C.; Yuan, Y.; Huang, J. Origin and Elimination of Photocurrent Hysteresis by Fullerene Passivation in CH3NH3PbI3 Planar Heterojunction Solar Cells.

Published on 12 February 2018. Downloaded on 12/02/2018 15:37:05.

Sustainable Energy & Fuels Accepted Manuscript

View Article Online
DOI: 10.1039/C7SE00545H

Nat. Commun. **2014**, *5*, 1–7.

(27) Kim, Y. C.; Jeon, N. J.; Noh, J. H.; Yang, W. S.; Seo, J.; Yun, J. S.; Ho-Baillie, A.; Huang, S.; Green, M. A.; Seidel, J.; Ahn, T. K.; Seok, S. Il. Beneficial Effects of PbI2 Incorporated in Organo-Lead Halide Perovskite Solar Cells. *Adv. Energy Mater.* **2016**, *6* (4).

(28) Kumar, V.; Schmidt, W. L.; Schileo, G.; Masters, R. C.; Wong-stringer, M.; Sinclair, D. C.; Reaney, I. M.; Lidzey, D.; Rodenburg, C. Nanoscale Mapping of Bromide Segregation on the Cross Sections of Complex Hybrid Perovskite Photovoltaic Films Using Secondary Electron Hyperspectral Imaging in a Scanning Electron Microscope. *ACS Omega* **2017**, *2*, 2126–2133.

(29) Okano, M.; Endo, M.; Wakamiya, A.; Yoshita, M.; Akiyama, H.; Kanemitsu, Y. Degradation Mechanism of Perovskite CH3NH3PbI3 Diode Devices Studied by Electroluminescence and Photoluminescence Imaging Spectroscopy. *Appl. Phys. Express* **2015**, *8* (10).

(30) Yuan, H.; Debroye, E.; Janssen, K.; Naiki, H.; Steuwe, C.; Lu, G.; Moris, M.; Orgiu, E.; Uji-I, H.; De Schryver, F.; Samorì, P.; Hofkens, J.; Roeffaers, M. Degradation of Methylammonium Lead Iodide Perovskite Structures through Light and Electron Beam Driven Ion Migration. *J. Phys. Chem. Lett.* **2016**, *7* (3), 561–566.

(31) Hentz, O.; Zhao, Z.; Gradečak, S. Impacts of Ion Segregation on Local Optical Properties in Mixed Halide Perovskite Films. *Nano Lett.* **2016**, *16* (2), 1485–1490.

(32) O'Kane, S. E. J.; Richardson, G.; Pockett, A.; Niemann, R. G.; Cave, J. M.; Sakai, N.; Eperon, G. E.; Snaith, H. J.; Foster, J. M.; Cameron, P. J.; Walker, A. B. Measurement and Modelling of Dark Current Decay Transients in Perovskite Solar Cells. *J. Mater.*

Published on 12 February 2018. Downloaded on 12/02/2018 15:37:05.

Sustainable Energy & Fuels Accepted Manuscript

View Article Online
DOI: 10.1039/C7SE00545H

Chem. C **2017**, *5* (2), 452–462.

(33) Calado, P.; Telford, A. M.; Bryant, D.; Li, X.; Nelson, J.; O'Regan, B. C.; Barnes, P. R. F. Evidence for Ion Migration in Hybrid Perovskite Solar Cells with Minimal Hysteresis. *Nat. Commun.* **2016**, *7*, 1–10.

(34) S. Meloni, T. Moehl, W. Tress, M. Franckevicius, M. Saliba, Y. H. Lee, P. Gao, M. K. Nazeeruddin, S. M. Zakeeruddin, U. Rothlisberger and M. GraetzelS. Meloni, T. Moehl, W. Tress, M. Franckevicius, M. Saliba, Y. H. Lee, P. Gao, M. K. Nazeeruddin, S. M. Za, U. R. and M. G. No Title. *Nat. Commun.* **2016**, *7*, 10334.

(35) Li, D.; Wu, H.; Cheng, H. C.; Wang, G.; Huang, Y.; Duan, X. Electronic and Ionic Transport Dynamics in Organolead Halide Perovskites. *ACS Nano* **2016**, *10* (7), 6933–6941.

(36) Gottesman, R.; Lopez-Varo, P.; Gouda, L.; Jimenez-Tejada, J. A.; Hu, J.; Tirosh, S.; Zaban, A.; Bisquert, J. Dynamic Phenomena at Perovskite/Electron-Selective Contact Interface as Interpreted from Photovoltage Decays. *Chem* **2016**, *1* (5), 776–789.

(37) Noh, J. H.; Im, S. H.; Heo, J. H.; Mandal, T. N.; Seok, S. Il. Chemical Management for Colorful, Efficient, and Stable Inorganic-Organic Hybrid Nanostructured Solar Cells. *Nano Lett.* **2013**, *13* (4), 1764–1769.

(38) Li, Z.; Yang, M.; Park, J. S.; Wei, S. H.; Berry, J. J.; Zhu, K. Stabilizing Perovskite Structures by Tuning Tolerance Factor: Formation of Formamidinium and Cesium Lead Iodide Solid-State Alloys. *Chem. Mater.* **2016**, *28* (1), 284–292.

(39) Saliba, M.; Matsui, T.; Seo, J.-Y.; Domanski, K.; Correa-Baena, J.-P.; Nazeeruddin, M. K.; Zakeeruddin, S. M.; Tress, W.; Abate, A.; Hagfeldt, A.; Grätzel, M. Cesium-Containing Triple Cation Perovskite Solar Cells: Improved Stability, Reproducibility and

Published on 12 February 2018. Downloaded on 12/02/2018 15:37:05.

Sustainable Energy & Fuels Accepted Manuscript

View Article Online
DOI: 10.1039/C7SE00545H

High Efficiency. *Energy Environ. Sci.* **2016**, *9* (6), 1989–1997.

(40) Weber, S.; Rath, T.; Mangalam, J.; Kunert, B.; Coclite, A. M.; Bauch, M.; Dimopoulos, T.; Trimmel, G. Investigation of NiOx-Hole Transport Layers in Triple Cation Perovskite Solar Cells. *J. Mater. Sci. Mater. Electron.* **2017**, *0* (0), 1–9.

Published on 12 February 2018. Downloaded on 12/02/2018 15:37:05.

Sustainable Energy & Fuels Accepted Manuscript

View Article Online
DOI: 10.1039/C7SE00545H

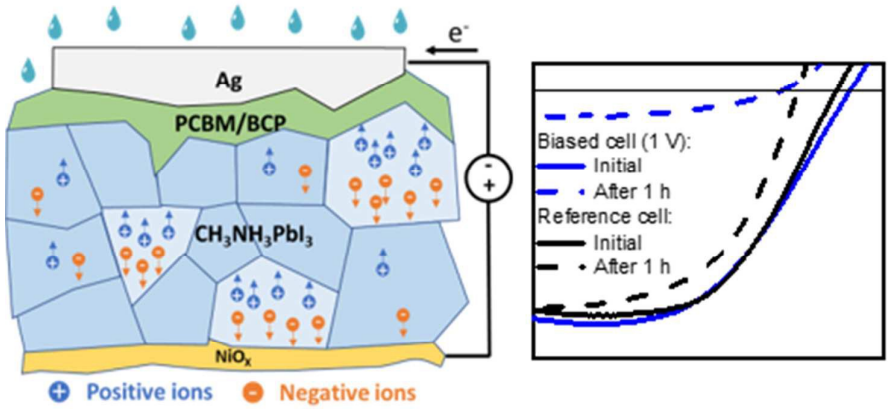

The dark electrical bias degradation of inverted perovskite solar cells is due to ion migration in presence of moisture

Published on 12 February 2018. Downloaded on 12/02/2018 15:37:05.

Sustainable Energy & Fuels Accepted Manuscript